phys. stat. sol. (b) **225**, No. 1, 135–143 (2001)

Characteristic Phonon Scattering Enhancement Correlated with Magnetic and Charge Orders in $La_{1-X}Sr_XMnO_3$ ($X \geq 0.50$)

M. IKEBE[1]), H. FUJISHIRO, S. KANOH, and T. MIKAMI[*])

Department of Materials Science and Technology, Faculty of Engineering, Iwate University, 4-3-5 Ueda, Morioka 020-8551, Japan

(Received September 11, 2000; in revised form December 8, 2000; accepted December 8, 2000)

Subject classification: 63.20.Dj; 66.70.+f; 72.15.Eb; 75.30.Kz; S10.15

The thermal conductivity $\kappa(T)$ and the thermal diffusivity $\alpha(T)$ of $La_{1-X}Sr_XMnO_3$ ($X \geq 0.50$) have been measured and phonon scattering mechanisms have been analyzed in terms of the power of dependence on phonon frequency ω_{ph}. For $0.50 \leq X < 0.55$, where the high temperature ferromagnetic phase becomes unstable against the A-type antiferromagnetic (AF) order, the phonon scattering mechanism proportional to ω_{ph}^1 is enhanced in the low temperature AF phase. In contrast, in the charge ordered phase for $X \geq 0.67$, the phonon scattering mechanism proportional to ω_{ph}^4 is enhanced. The enhancement in the phonon scattering mechanisms reflects the types of the order in this manganese system.

1. Introduction

A series of carrier doped manganites with the formula $RE_{1-X}AE_XMnO_3$ (RE: lanthanide, AE: alkaline earth ions) show a variety of dramatic physical properties on the stage of the Mott metal–insulator transition. The dramatic properties result from competition or cooperation of various interactions such as the ferromagnetic double exchange, antiferromagnetic superexchange, charge ordering, orbital ordering, static and dynamic Jahn-Teller effect and structural instability etc. From theoretical [1] and experimental [2–7] investigations, it has been widely recognized that, besides the double exchange interaction, the electron-lattice coupling is important to determine the transport properties. The electrical transport has been extensively and intensively studied, while the thermal transport has not been so systematically investigated [8–11]. Because the electrical resistivity $\varrho(T)$ of $La_{1-X}Sr_XMnO_3$ is pretty large even in the ferromagnetic metallic phase, the heat conduction is overwhelmingly due to phonons. The phonon scattering in the manganite compound is expected to show uncommon features because the lattice system is also under a strong influence of the various interactions which cause uncommon properties of the electron system.

$La_{1-X}Sr_XMnO_3$ (LSMO) exhibits various magnetic and charge order phenomena for $X \geq 0.50$. Our previous studies for the electrical resistivity $\varrho(T)$ [12], the magnetization $M(T)$ [13] and the sound velocity anomaly [12] have clarified the following characteristics of the phase diagram of LSMO. LSMO ($X = 0.48$) is a ferromagnet with $T_c = 320$ K. For $X = 0.50$ and 0.55, the high temperature ferromagnetic (FM) phase becomes unstable against the layer-type (A-type) antiferromagnetic (AF) order. The A-type AF

[1]) Tel.: +81-19-621-6362; FAX: +81-19-621-6373; e-mail address: ikebe@iwate-u.ac.jp
[*]) Present address: Nippon System Ware Co. Ltd., Sakuragaoka, Shibuya-ku, Tokyo 150-0031, Japan.

order is stabilized below T_N for $0.50 \leq X \leq 0.60$ in the LSMO system [12–14]. It is to be noticed that the A-type AF order is not compatible with the charge order (CO) phase [15]. The CO transition takes place for $X = 0.67$ and $X = 0.75$, possibly concomitant with the C-type AF order [16]. We have already reported an anomalous phonon scattering mechanism operating in LSMO ($X \approx 0.17$) compounds around the ferromagnetic ordering temperature T_c [11]. For these compounds, the strong phonon scattering around T_c was pointed out to originate from dynamical structural fluctuations correlated with critical spin fluctuations. We have also pointed out a two-level-like dynamical scattering mechanism which may operate in LSMO for $X \approx 0.125$, where the charge order related to the polaron localization occurs [17]. In the present paper, we report enhanced phonon scattering mechanisms characteristic of the type of ordering in $La_{1-X}Sr_XMnO_3$ system for $X \geq 0.50$.

2. Experimental

$La_{1-X}Sr_XMnO_3$ samples were prepared from stoichiometric mixtures of La_2O_3, $SrCO_3$ and Mn_3O_4 powders. The mixtures were calcined twice at 1000 °C for 24 h in air, pressed into pellets and sintered at 1500 °C for 8 h in air. The pellets were heat-treated at 1500 °C for 24 h in O_2 gas flow. The densities of the samples, which were determined by measuring the volume and weight, were higher than 80% of ideal ones. All the samples were confirmed to be in a single phase by X-ray diffraction at room temperature. The thermal conductivity $\kappa(T)$ was automatically measured by a steady state heat flow method between 10 and 300 K, using a Gifford-McMahon cycle helium refrigerator as a cryostat [18]. The thermal diffusivity $\alpha(T)$ was measured by an arbitrary heating method under the same experimental setup as the $\kappa(T)$ measurement.

3. Experimental Results

Figures 1 to 4 show the temperature dependence of the phonon thermal conductivity κ_{ph} and the phonon thermal diffusivity α_{ph} ($= \kappa_{ph}/C$, C specific heat) of LSMO for $X = 0.48$, 0.50, 0.60 and 0.67 as typical samples. The electronic contribution, κ_e and α_e, estimated from the Wiedemann-Franz law is negligibly small except for $X = 0.48$. In Fig. 1, for ferromagnetic LSMO ($X = 0.48$), κ_e (which is at most 2% of the total κ) is

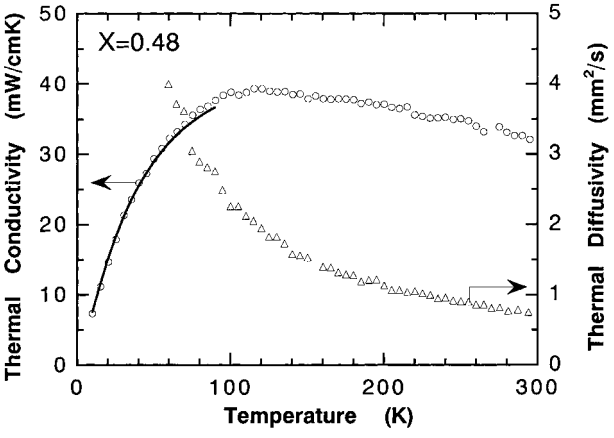

Fig. 1. The thermal conductivity $\kappa(T)$ and the diffusivity $\alpha(T)$ as a function of T for $La_{1-X}Sr_XMnO_3$ ($X = 0.48$). The solid line (10 K $\leq$ T $\leq$ 90 K) is the calculated fitting curve for κ(T) (see text)

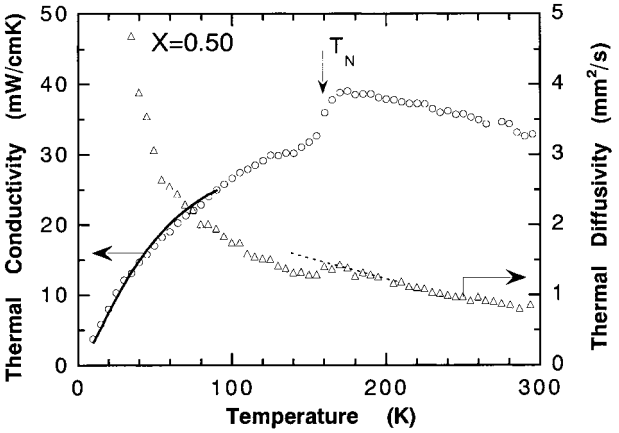

Fig. 2. κ(T) and α(T) of LSMO for $X = 0.50$, which are sharply depressed at the onset of the A-type antiferromagnetic order at T_N. The solid line is the fitting curve

subtracted from the measured κ to obtain κ_{ph}. In Figs. 2 and 3, the arrow indicates the Néel temperature T_N and in Fig. 4, the arrow represents the CO temperature T_{CO} ($= T_N$) determined from $\varrho(T)$, $M(T)$ or the sound velocity $v_s(T)$ [13].

With decreasing temperature, κ_{ph}(T) of LSMO ($X = 0.50$) in Fig. 2 shows a clear and sharp reduction around T_N. This sample shows the FM order at $T_c \approx 290$ K, which gives place to the A-type AF order below $T_N \approx 160$ K [12, 13]. κ_{ph} of LSMO ($X = 0.52$) shows the similar behavior, though the reduction at T_N is considerably smaller (not shown in the figure). It is to be noticed that the FM to AF transition is of first order with hysteresis. The reduction of κ_{ph} suggests an enhancement in the phonon scattering or the appearance of a new scattering mechanism. The corresponding decrease in κ_{ph} ($= v_s^2\langle\tau_{ph}\rangle/3$, $\langle\tau_{ph}\rangle$ average phonon scattering time) around T_N can also be seen in Fig. 2, which more directly demonstrates the phonon scattering enhancement. $\kappa_{ph}(T)$ and $\alpha_{ph}(T)$ of LSMO ($X = 0.67$) in Fig. 4, also show a reduction around T_{CO}. In contrast, $\kappa_{ph}(T)$ of LSMO ($X = 0.60$) in Fig. 3 shows a broad shallow dip around T_N. This dip in κ_{ph}(T) is indicative of the phonon scattering enhancement through some dynamical mechanism related to the critical spin fluctuations around the second order magnetic phase transition in this compound.

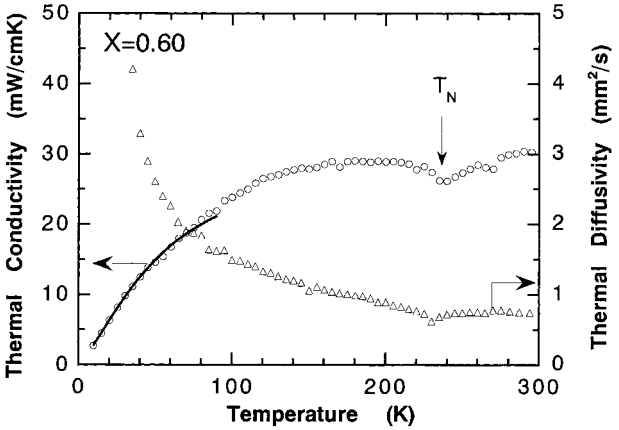

Fig. 3. κ(T) and α(T) of LSMO for $X = 0.60$. The phonon scattering enhancement is noticeable around T_N. The solid line is the fitting curve

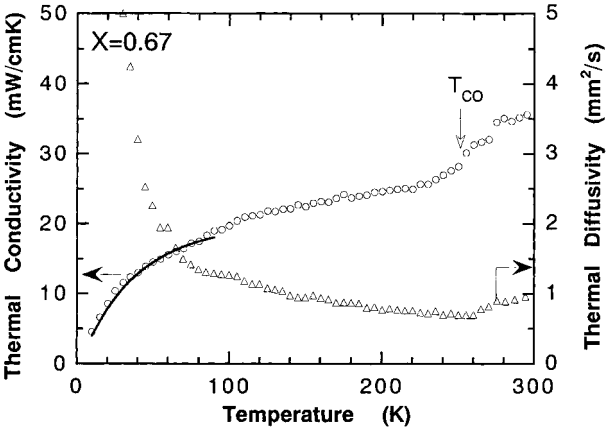

Fig. 4. κ(T) and α(T) of LSMO for $X = 0.67$. The phonon scattering is strongly enhanced below and above the charge order temperature T_{CO}. The solid line is the fitting curve

As we have seen, the AF transition and the CO transition accompany the scattering enhancement in LSMO. Including the data on other samples not presented in the figures, the effects of AF order and CO for $X \geq 0.50$ are summarized as follows: (i) For $0.50 \leq X < 0.55$, where the FM order becomes unstable against the low temperature A-type AF phase, the phonon scattering enhancement appears rather sharply at T_N and the enhancement occurs over the whole temperature range below T_N. (ii) For $0.55 \leq X \leq 0.60$, where the A-type AF phase is dominant and the FM order is absent or not influential, the phonon scattering enhancement occurs only in the critical region around T_N and is not so significant at low temperatures. (iii) For $0.67 \leq X \leq 0.75$, the charge order accompanied by the C-type AF order strongly enhances the phonon scattering again over the whole temperature range below T_{CO}. The enhancement appears rather gradually at a temperature somewhat higher than T_{CO}. In the following section, we analyze the phonon scattering mechanisms operative in each ordered phase.

4. Discussion

On the basis of the relaxation time method [19], the phonon thermal conductivity is given by

$$\kappa_{ph} = \frac{3dnRT^3}{M\Theta_D^3} v_s^2 \int_0^{\Theta_D/T} \frac{x^4 e^x}{(e^x - 1)^2} \tau_{ph} \, dx \,, \tag{1}$$

where d is the mass density, M the weight of one mole, n the number of atoms in the chemical formula of the compound ($n = 5$ for $La_{1-X}Sr_XMnO_3$), R the gas constant, Θ_D the Debye temperature and x ($= \omega_{ph}/T$) is the reduced phonon frequency. Assuming a kind of Matthiessen's rule for the phonon scattering rate, the phonon relaxation time τ_{ph} is given by (see, e.g., [19])

$$\tau_{ph}^{-1} = \tau_b^{-1} + KTx + sT^2x^2 + pT^4x^4 \,. \tag{2}$$

Here, τ_b is the scattering time due to grain boundaries and the K, s and p terms represent the phonon scattering strength proportional to ω_{ph}^1, ω_{ph}^2 and ω_{ph}^4, respectively. It is to be noticed that, with increasing power of ω_{ph}, the corresponding scattering becomes

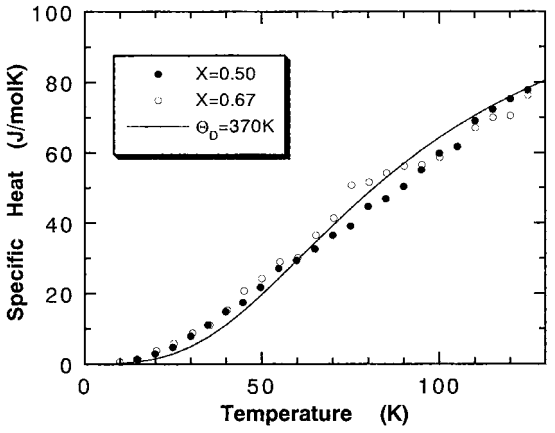

Fig. 5. The estimated specific heat C by use of the relation $C = \kappa/\alpha$. The solid line represents the Debye specific heat for the Debye temperature $\Theta_D = 370$ K

relatively more efficient in a higher temperature region. The standard theory of the phonon scattering [20] refers to the K term as the phonon scattering by the strain fields around dislocations and to the s and p term as the phonon Rayleigh scattering by sheet-like faults and point defects, respectively. In order to analyze the phonon scattering on the basis of eqs. (1) and (2), we need the Θ_D value of $La_{1-X}Sr_XMnO_3$. Since we have measured both κ and α, the specific heat C (per unit volume) can be estimated by the relation $C = \kappa/\alpha$. Figure 5 shows the estimated specific heat of LSMO for $X = 0.50$ and 0.67. As can be seen, the magnitudes of the specific heat of both specimens (and of other samples not shown in the figure) are roughly consistent with the Debye specific heat line with $\Theta_D = 370$ K. So we set the Θ_D value to be 370 K for all the present $La_{1-X}Sr_XMnO_3$ compounds. In the estimation of Θ_D, the electronic contribution to the specific heat was neglected because the carrier density is low and the fitting with the Debye curve was performed in a rather high temperature range (30 K < T < 90 K). The phonon scattering time by boundaries τ_b is set to satisfy the relation $l_b = \tau_b v_{ph}$, where l_b is the average size of the grains. The size of l_b was determined to be 5 μm $\leq l_b \leq$ 40 μm by a scanning electron microscope and v_{ph} was determined by the ultrasonic pulse superposition method [12]. Actually, the grain boundary scattering is almost neglectable in the temperature range of the present work (T > 10 K) because other scattering mechanisms are by far dominant. By using eqs. (1) and (2), κ_{ph} was calculated to best fit the experimental data with K, s and p values as adjustable parameters. The fitting temperature region was selected between 10 and 90 K. It is to be noticed that the ω_{ph} power law of τ_{ph} given by eq. (2) is valid only for temperatures well below Θ_D and the fitting temperature region satisfies the condition,

Table 1

Summary of the parameters determined in the κ_{ph} fitting processes in $La_{1-X}Sr_XMnO_3$ samples on the basis of eqs. (1) and (2)

sample	d (g/cm^3)	v_s (10^5 cm/s)	τ_b^{-1} (10^8 s^{-1})	l_b (μm)	s (10^8 K^{-2}s^{-1})	p (10^4 K^{-4}s^{-1})	K (10^9 K^{-1}s^{-1})
$X = 0.48$	5.67	4.15	2.6	37	0.41	0.28	0.11
$X = 0.50$	5.50	5.16	2.6	30	1.0	0.29	1.7
$X = 0.60$	5.45	5.23	7.2	14	1.5	0.29	1.1
$X = 0.67$	5.49	5.72	7.0	14	1.5	1.3	0.41
$X = 0.17$	5.28	4.30	2.2	45	0.5	0.76	1.1

$T < \Theta_D/4$ [20]. The results of the fitting for κ_{ph} are given in Figs. 1 to 4 by solid lines and the parameter values determined are summarized in Table 1, together with the results for another concentration X not shown in the figures.

In order to clearly see the contributions of each scattering mechanism, the total phonon scattering rate and the scattering rates of each scattering term were calculated as an average over the Debye phonon spectrum. The results are given in Figs. 6a–d for $X = 0.48$, 0.50, 0.60 and 0.67. The total scattering rate $\langle\tau_{ph}\rangle_t^{-1}$ was calculated by use of the following equation and the parameter values in Table 1:

$$\langle\tau_{ph}\rangle^{-1} = \frac{\int_0^{\Theta_D/T} \tau_{ph} \frac{x^4 e^x}{(e^x-1)^2}\,dx}{\int_0^{\Theta_D/T} \frac{x^4 e^x}{(e^x-1)^2}\,dx}. \quad (3)$$

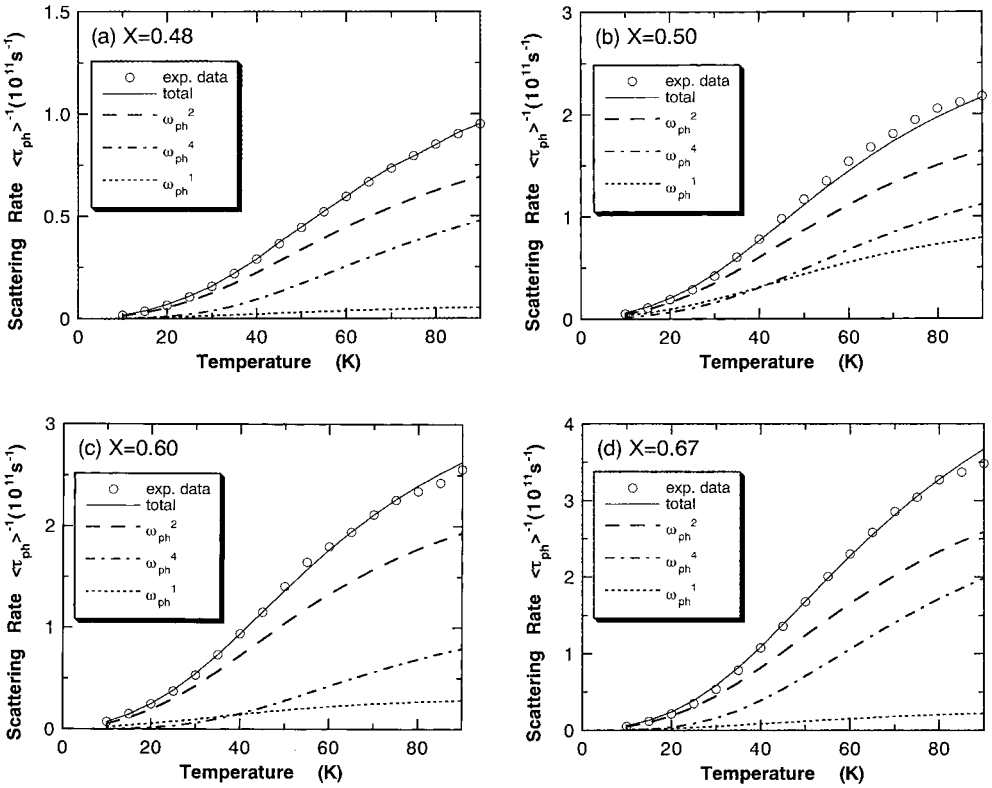

Fig. 6. Calculated phonon scattering rate $\langle\tau_{ph}\rangle^{-1}$ and contributions of the scattering terms proportional to ω_{ph}^1 (K term), ω_{ph}^2 (s term), and ω_{ph}^4 (p term) for LSMO samples with a) $X = 0.48$, b) $X = 0.50$, c) $X = 0.60$ and d) $X = 0.67$. The contributions of each scattering term were estimated assuming that the every scattering term was completely removed (see text). Open circles are experimental points corresponding to the observed thermal conductivity $\kappa(T)$

It is to be noticed that the total scattering rate is inversely proportional to the measured phonon thermal diffusivity α_{ph} ($= v_s^2 \langle \tau_{ph} \rangle / 3$) if the sound velocity v_s is assumed temperature independent. The contributions of the K, s and p terms, $\langle \tau_{ph} \rangle_{K,s,p}^{-1}$, were obtained by calculating $\langle \tau_{ph} \rangle$ on the assumption that the corresponding term is removed and subtracting $\langle \tau_{ph} \rangle^{-1}$ from the total $\langle \tau_{ph} \rangle_t^{-1}$. On the basis of a number of trials, each parameter value was reproducible within $\pm 5\%$ of the total scattering rate $\langle \tau_{ph} \rangle^{-1}$.

Comparing Figs. 6a and b, we notice that the K-term (ω_{ph}^1) contribution is appreciable for LSMO ($X = 0.50$), in contrast to the very small, almost negligible K-term contribution for ferromagnetic LSMO ($X = 0.48$). As we have previously mentioned, a standard origin of K-term scattering is due to the strain fields around dislocations. In the present LSMO ($X = 0.50$), however, it is unlikely that the A-type AF order causes a drastic increase of dislocations and the other phonon scattering mechanism must be operative below T_N. Another scattering mechanism which has approximately the same ω_{ph}^1 dependence is due to tunneling states. The thermal dilatation dL/L of LSMO ($X = 0.50$) displays a sharp contraction at T_N with decreasing temperature [12]. This result suggests an appreciable lattice change associated with the FM to AF transition in this compound. In the previous paper [17] we pointed out a possibility of strong phonon tunneling scattering associated with the polaron order in LSMO for $X \leq 0.18$. The lattice site tunneling of oxygen, the most light atom composing LSMO, was considered to be important for the phonon scattering. Because the FM and AF orders in $La_{0.50}Sr_{0.50}MnO_3$ accompany different lattice states through the strong spin–lattice interaction, a kind of two-level phonon scattering associated with spin fluctuation may be possible in this compound. The scattering rate due to the two-level tunneling states is expressed as $ATx \tanh(x/2)$ [21]. On the basis of the Debye phonon spectrum, the dominant phonon frequency ω_d at temperature T is given by $\hbar\omega_d = 1.6 k_B T$ and the term $ATx \tanh(x/2)$ is approximately equal to $ATx \tanh(0.8) = 0.67\, ATx$, thus giving the same ω_{ph}^1 dependence as the K term in eq. (2). We propose that the appearance of K-term scattering in LSMO ($X = 0.50$) is due to the phonon scattering by lattice tunneling states which originates from the oxygen site tunneling correlated with FM and AF order fluctuations.

Comparing the scattering strength of LSMO ($X = 0.67$) in Fig. 6d to LSMO ($X = 0.50$), we notice that the K-term scattering is weakened and the p-term component is enhanced in this CO phase sample. Contrary to the A-type antiferromagnet LSMO ($X = 0.50$), the lattice of LSMO ($X = 0.67$) shows expansion around T_{CO} with decreasing temperature [12] and there is a difference between the lattice states of the A-type AF and the CO with C-type AF phases. Several recent investigations reported an enhancement of the Jahn-Teller distortion below the charge order onset temperature T_{CO}. The p-term scattering proportional to ω_{ph}^4 is usually ascribed to the scattering by point-type defects. If we literally follow this rule, the charge ordering should enhance the point defect scattering. This may be possible if CO enhances the local incoherent Jahn-Teller distortion around Mn^{3+} ions, though we cannot point out the exact origin of the enhancement at the present stage. The strong p-term scattering at low temperatures, is one of the characteristic features of the phonon scattering in the CO phase samples.

Another characteristic feature of the phonon scattering enhancement in the CO phase sample can be seen at high temperatures. In Fig. 4, both the conductivity $\kappa(T)$ and the diffusivity $\alpha(T)$ of LSMO ($X = 0.67$) clearly decrease at higher temperatures than its T_{CO}. The similar behavior was observed also for LSMO ($X = 0.75$). Recent

extensive studies [21, 22] have shown that dynamic charge correlation is important in these Mott insulators above T_{CO}. The enhanced phonon scattering above T_{CO} is indicative of the importance of a dynamical phonon scattering mechanism related to the charge order fluctuation.

Although the enhanced K-term scattering provides a peculiarity of the A-type AF state and the enhanced p-term scattering makes a peculiarity of the CO state accompanied with the C-type AF order, the s-term component is always dominant in Figs. 6a–d. Especially in Fig. 6c, the scattering strength of both K and p term is weak for LSMO ($X = 0.60$) and the s term is overwhelmingly dominant. This compound directly enters into (possibly the A-type) AF order not showing the intermediate FM order. The dilatation dL/L displays very slight contraction at T_N [12]. Then the lattice effect may not be influential in this compound, which is possibly consistent with relatively small K-term and p-term scattering. The s-term scattering, which is proportional to ω_{ph}^2, usually comes from two-dimensional-like lattice defects such as stacking faults, twin boundaries, etc. The microscopic origin for the s-term scattering is not clear either, but the dominant s-term scattering provides another peculiarity of the phonon scattering in the $La_{1-X}Sr_XMnO_3$ system as a whole.

5. Summary

The phonon thermal conductivity κ_{ph} and the thermal diffusivity α_{ph} of $La_{1-X}Sr_XMnO_3$ were measured for the nonmetallic region of the Sr concentration X (≥ 0.50) and the phonon scattering mechanisms were analyzed in terms of the power of dependence on phonon frequency ω_{ph}. The A-type antiferromagnetic order and the charge order accompanied with the C-type AF order resulted in an enhancement of the characteristic phonon-scattering mechanisms. The phonon scattering proportional to ω_{ph}^1 was enhanced in $La_{0.50}Sr_{0.50}MnO_3$ (A-type AF) and we proposed that the phonon scattering due to tunneling states related to lattice instability might be important in $La_{0.50}Sr_{0.50}MnO_3$. In contrast, the phonon scattering proportional to ω_{ph}^4 was enhanced in the charge ordered C-type AF phase of $La_{0.33}Sr_{0.67}MnO_3$. The enhanced local Jahn-Teller distortion might be responsible for the enhancement in the ω_{ph}^4 phonon scattering. Thus, in the $La_{1-X}Sr_XMnO_3$ system the different type of ordering brings about a phonon scattering enhancement characterized by different power dependence on phonon frequency ω_{ph}.

References

[1] A.J. MILLIS, B.I. SHRAIMAN, and R. MUELLER, Phys. Rev. Lett. **77**, 175 (1996).
[2] A. ASAMITSU, Y. MORITOMO, Y. TOMIOKA, T. ARIMA, and Y. TOKURA, Nature **373**, 407 (1995).
[3] H.Y. HUANG, S-W. CHEONG, P.G. RADAELLI, M. MAREZIO, and B. BATLOGG, Phys. Rev. Lett. **75**, 914 (1995).
[4] P. DAI, J. ZHANG, H.A. MOOK, S-J. LIOU, P.A. DOWBEN, and E.W. PLUMMER, Phys. Rev. B **54**, 3694 (1996).
[5] S.J.L. BILLINGE, R.G.DiFRANCESCO, G.H. KWEI, J.J. NEUMEIR, and J.D. THOMPSON, Phys. Rev. Lett. **77**, 715 (1995).
[6] G. ZHAO, K. CONDER, H. KELLER, and K.A. MÜLLER, Nature **381**, 676 (1996).
[7] H. KAWANO, R. KAJIMOTO, M. KUBOTA, and H. YOSHIZAWA, Phys. Rev. B **53**, R14709 (1996).
[8] D.W. VISSER, A.P. RAMIREZ, and M.A. SUBRAMANIAN, Phys. Rev. Lett. **78**, 3947 (1997).
[9] J.L. COHN, J.J. NEUMEIER, C.P. POPOVICIU, K.J. McCLELLAN, and TH. LEVENTOURI, Phys. Rev. B **56**, R8495 (1997).

[10] J. Hejtmanek, Z. Jirak, Z. Arnold, M. Marysko, S. Krupicka, C. Martin, and F. Damay, J. Appl. Phys. **83**, 7204 (1998).
[11] M. Ikebe, H. Fujishiro, and Y. Konno, J. Phys. Soc. Jpn. **67**, 1083 (1998).
[12] H. Fujishiro, T. Fukase, and M. Ikebe, J. Phys. Soc. Jpn. **67**, 2582 (1998).
[13] H. Fujishiro, M. Ikebe, and Y. Konno, J. Phys. Soc. Jpn. **67**, 1799 (1998).
[14] T. Akimoto, Y. Maruyama, Y. Moritomo, A. Nakamura, K. Hirota, K. Ohoyama, and M. Ohashi, Phys. Rev. B **57**, 1 (1998).
[15] H. Kawano, R. Kajimoto, H. Yoshizawa, Y. Tomioka, H. Kuwahara, and Y. Tokura, Phys. Rev. Lett. **78**, 4235 (1997).
[16] E.O. Wollan and W.C. Koeher, Phys. Rev. **100**, 545 (1955).
[17] H. Fujishiro and M. Ikebe, Physica B **263/264**, 691 (1999).
[18] M. Ikebe, H. Fujishiro, T. Naito, and K. Noto, J. Phys. Soc. Jpn. **63**, 3107 (1994).
[19] R. Berman, Thermal Conduction in Solids, Clarendon Press, Oxford/New York 1976.
[20] P.G. Klemens, Solid State Physics, Eds. F. Seitz and D. Turnbull, Vol. 7, Academic Press, New York 1958.
[21] S-W. Cheong and C.H. Chen, in: Colossal Magnetoresistance, Charge Ordering and Related Properties of Manganese Oxides, Eds. C.N.R. Rao and B. Raveau, World Scientific, Singapore 1998.
[22] J. Zaanen, Science **286**, 251 (1999).